Meyniana	53	Seite 143–162	9 Abb.	Kiel, (Sept.) 2001

Style and rate of shelf sedimentation offshore Nha Trang, Vietnam, South China Sea

WITOLD SZCZUCIŃSKI & KARL STATTEGGER

SZCZUCIŃSKI, WITOLD; STATTEGGER, KARL, 2001: Style and rate of shelf sedimentation offshore Nha Trang, Vietnam, South China Sea. {Sedimentation und Sedimentationsraten in der Schelfregion von Nha Trang, Vietnam, Südchinesisches Meer}.– Meyniana, **53**:143–162, 9 fig., Kiel.

The offshore region of Nha Trang, southern Vietnam, was investigated to determine conditions, rates and processes of modern sedimentation. Seismic surveys, X-ray radiography, granulometry, magnetic susceptibility, coarse fraction analysis and mineralogic composition, carbon and heavy metal contents and ^{210}Pb dating of gravity- and box-core material were carried out.

The inner shelf is up to 40 m deep and is characterised by reworking and bypassing of sediment. The middle shelf is dominated by an up to 40 m thick clastic sediment wedge down to a water depth of about 100 m. The outer shelf shows several small basins below 100 m water depth.

Modern sediments are generally fine-grained. The sand fraction (less than a few percent) consists almost entirely of carbonate skeleton particles of shells, foraminifers etc., and lithoclasts, mostly mica and quartz. The sediments are homogeneous and strongly bioturbated with some relicts of primary stratification, which suggest non-steady sedimentation. The organic carbon content is about 1% and increases shoreward. Pb, Cr, and Cu contents are highest in the nearshore surface sediments.

The sedimentation rate estimated on ^{210}Pb dating reveals values between 0.33 – 0.37 cm/yr at 92 m and 103 m water depth.

Most of the material is delivered from the short mountain rivers reaching Nha Trang Bay. In the inner shelf area, intensive reworking is caused by high-energetic action of waves and tidal currents. In the deeper parts, the influence of biogenic activity is increasing in form of bioturbation and production of carbonates.

W. SZCZUCIŃSKI, M. Sc., Institute of Geology, Adam Mickiewicz University, ul. Maków Polnych 16, 61-686, Poznań, Poland and Collegium Polonicum, ul. Kościuszki 1, 69-100, Słubice, Poland,
Email: Witold.Szczucinski@euv-frankfurt-o.de
Prof. Dr. K. STATTEGGER, Institut für Geowissenschaften, Christian-Albrechts-Universität, D-24098 Kiel, Germany. Email:ks@gpi.uni-kiel.de.

Kurzfassung

In der Schelfregion von Nha Trang, Süd-Vietnam, wurden die heutigen Sedimentationsprozesse und Sedimentationsraten untersucht. Die verwendeten Methoden umfassen reflexionsseismi-

sche Untersuchungen, Radiografie, Korngrößenanalyse, Komponentenanalyse (einschl. Mineralbestimmung), magnetische Suszeptibilität, Schwermetall-Geochemie, C_{org}-Bestimmung und ^{210}Pb Datierungen an Schwerelot- und Großkastengreiferproben.
Im Untersuchungsgebiet lässt sich der Schelf in drei Gebiete einteilen. Der innere Schelf weist Tiefen bis zu 40 m auf und ist durch umgelagerte Sedimente, verbunden mit intensivem Sedimenttransport, charakterisiert. Der mittlere Schelf wird von einem klastischen Sedimentfächer dominiert, der bis in Wassertiefen von 100 m hinabreicht. Sedimente des äußeren Schelf wurden in mehreren kleinen morphologischen Depressionen unterhalb von 100 m Wassertiefe gefunden.
Der Hauptanteil der jungen Sedimentbedeckung umfasst feinklastische Sedimente der Silt- und Tonfraktion. Die Sandfraktion, die sich auf wenige Prozent beschränkt, besteht nahezu ausschließlich aus karbonatischem Material, wie Schalenbruchstücken und Foraminiferen sowie Lithoklasten (Glimmer und Quarz). Die Sedimente sind stark verwühlt, weisen vereinzelt aber noch Reste von Schichtung auf, was auf wechselhafte Sedimentationsbedingungen hindeutet. Der C_{org}-Anteil beläuft sich auf ca. 1% und nimmt zur Küste hin zu. Der Pb-, Cr-, und Cu-Gehalt ist am größten in den Oberflächensedimenten im Küstengewässer. Die Abschätzung der Sedimentationsrate mit Hilfe von Pb^{210}-Datierungen ergab 0.33–0.37 cm pro Jahr in 92 m und 103 m Wassertiefe.
Kleine Flüsse, die ihren Ursprung in der Bergregion des Hinterlandes haben, sind die Hauptzulieferer des Sedimentmaterials der Bucht von Nha Trang. Die Ablagerungen des inneren Schelfs sind aufgrund von intensiver Wellenaktivität sowie tidalen Strömungen stark aufgearbeitet und umgelagert. In tieferen Bereichen nimmt der Einfluss von biologischer Aktivität in Form von Bioturbation und Karbonatproduktion zu.

Introduction

The South China Sea (SCS) is one of the most intensively studied Asian seas. Much effort was given in understanding Quaternary evolution and paleoceanography of the SCS, but most workers have concentrated on deep sea sediments (Wang et al. 1999) or on wide shelf areas of the Sunda Shelf (Hanebuth et al. 2000) and off the Chinese coast. Very little sedimentological work has been done in the central part of Vietnam Shelf up to recent times. Su & Wang (1994) presented basic characteristics of modern sediments in SCS. According to this study, in our area of interest, sand and silty clay are accumulated that belong to the neritic facies of the inner and outer shelf. Considering the genetic types, they classified sediments on the shelf in the vicinity of Nha Trang as nearshore terrigenous sands and silts.

Even less is known about modern sedimentation rates in SCS. Some calculations based mostly on radiocarbon dating deal with averaged rates for periods of several thousands of years (e.g. Hanebuth 2000). Experiments with sediment traps have been carried out in deep part of SCS (Wiesner et al. 1996).

Our goals in the offshore region of Nha Trang in southeastern Vietnam are:

– to map the sediment types in the area

– to determine the modern sedimentation rate and to find out which are the dominant processes of sedimentation.

The study was supported by the German Federal Ministry of Education and Research (Grant Nos. 03G0140A and B). The research was also a contribution in the Master Course in Coastal Geosciences and Engineering at the Christian Albrecht University in Kiel. Supported also by *Europa Fellows* fellowship to W. Szczuciński. The authors would like to thank Martina Arp, Thomas Arpe, Carl-Dieter Garbe-Schönberg, Till Hanebuth, Ove Krüger, Stanisław Lorenc, Ludvig Löwemark, Boghardt Meier, Charu Sharma, Alexander Schimanski, Jan Scholten, Stephan Steinke, and the whole scientific and nautical crew working during the SONNE 140 cruise.

Study area

The study area is located at the western margin of SCS (fig. 1) and belongs to the coastal and shelf area off southeastern Vietnam. It is situated between 109°18.5' E and 109°32.5' E, and 12°12' N and 12°15' N.

Mountainous relief reaching several hundred meters in altitude only a few km from the coast controls the topography of the hinterland. The general strike of the main ranges is north-south, with several branches striking NWW–SEE in the east. They form the watershed between the Mekong catchment and small rivers flowing to the east. On the coast, they build peninsulas

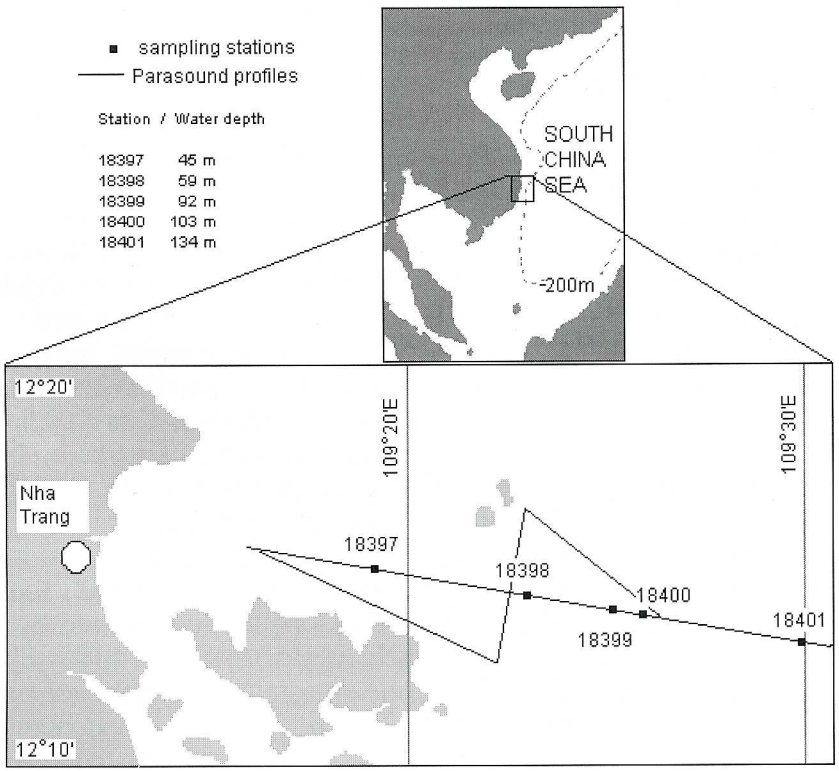

Fig. 1: Location of the study area, sampling stations and Parasound profile-tracks.

and islands with small alluvial plains and bays located inbetween, such as Nha Trang Bay (fig. 1). Most of the coastline in this region is rocky, and sandy beaches or tidal flats are found only inside the bays where alluvial plains developed.

Nha Trang Bay forms a shallow embayment with depths between 10 to 20 m. In the eastern entrance (about 20 km offshore), it is 35 m to 45 m deep. The shelf area is the narrowest in the whole SCS, and is about 40 km wide. It slope inclines an average of 0.24° between 30 m and 200 m depth. The continental slope from 200 m to 2000 m is much steeper with slopes about 2.29°.

The studied region is located at the borders of the Sundaland continental plate and is assumed to be tectonically stable during the Quaternary (Tjia & Liew 1996). An important dislocation, termed the 110°-Fault runs parallel to the Vietnam Coast, and cuts across the study area. Two fault zones in the region of Nha Trang trending SW–NE join the 110°-Fault (Fontaine & Workman 1997). The coast to the north of Nha Trang consists mainly of gneisses, schists, amphibolites and granites of the Kontum Massif, but younger intrusive rocks such as granites and intermediate to acidic volcanics are also present. Granite dominates in the vicinity of Nha Trang Bay. To the south, the shoreline is composed of alluvial deposits (Fromaget et al. 1952; Fontaine & Workman 1997). Volcanic activity persisted during Tertiary and Quaternary times and was mainly of basaltic and basanitic type. The last large eruption was noted in 1923 in the area of the Catwick Islands, some 200 km to the south from Nha Trang Bay (Simkin et al. 1981).

The Quaternary style of marine deposition was controlled by sea level fluctuations. From reconstructions made on the Sunda Shelf (Hanebuth 2000; Hanebuth et al. 2000), it is known that during the last glacial lowstand (20 to 22 cal kyr BP), sea level dropped by about –120 m. The succeeding sea level rise was not uniform and, in part, highly accelerated during short periods. During the Holocene optimum (6000–5000 years BP) sea level was even a few meters higher than at present (Tjia 1980, Davis et al. 2000).

The climate of the region is mostly influenced by the monsoon cycle, and belongs to the humid and warm tropical zone. Monsoon climate is basically characterised by two distinct seasons in the year, although higher ranges of climatic periodicity were found as well (Fairbridge 1986). The summer season is associated with dominant southwest winds and heavy rainfalls reaching 1000 mm/year. Divergences from this general pattern are caused by topographical factors, and are also attributed to climatic forcings such as El Niño.

The monsoon regime develops typical sea-surface current patterns. Several field studies (e.g. Wyrtki 1961; Huang et al. 1994b), and numerical-modelling experiments (e.g. Shaw & Chao 1994) reveal that the prevailing winter monsoon results in a cyclonic circulation of the surface layer, while the

prevailing summer monsoon follows an anti-cyclonic circulation pattern. As a result, in almost all parts of SCS at least two opposite current directions can be observed, but there are some exceptions as in our study area. Although the whole system is switching, the northward directed currents are dominant over the whole year providing an important implication for sediment transport. The study area is characterised by mesotidal conditions with tidal ranges is up to 2.5 m during spring tides (PIRAZZOLI 1991; HUANG et al. 1994a; VIETNAM: POINTE LAGAN TO CAP VARELLA 1997). The tide may be diurnal (VIETNAM: POINTE LAGAN TO CAP VARELLA 1997) or mixed (HUANG et al. 1994a).

Along the Vietnamese coast, the giant Mekong and Red rivers are commonly assumed to transport most sediments to the SCS (MILLIMAN & MEADE 1983; DEPETRIS 1996). There is still not enough available data to answer how the sediment delivered by these big rivers are dispersed. Along the coast of Vietnam, there are also several short rivers. There is, on the other hand, convincing evidence that sediment discharge from small mountainous rivers is generally underestimated (MILLIMAN & SYVITSKI 1992). To Nha Trang Bay, three such rivers are delivering sediment: Song Cay and Song Cho in the northern part, and Song Cai in the locality of Nha Trang City.

Methods

All material was collected in April 1999 during the research cruise SO-140 with R/V SONNE. Sampling stations were selected on the basis of previously obtained profiles with PARASOUND shallow seismics (WIESNER et al. 1999). Bottom sediments were sampled by the large spade Giant Box Corer (GBC) and Gravity Corer (GC). Sediments from both corers were described, sampled and measured with Multi-Sensor Core Logger (MSCL/016) for magnetic susceptibility on board. X-ray radiographs were made from sediment slabs taken from GBC subcores (25 cm long, 10 cm wide, and 0.5 cm thick) by exposing to X-rays of low voltage (35 kV) for a few minutes (time dependant on water content of the sediment). Grain size composition of samples was investigated by wet sieving for the sand fraction and laser grain size analysis for the fine fraction ($<63\ \mu m$) with a GALAI-Laser-Granulometer.

Coarse grain analyses were performed for $>250\ \mu m$, and $125-250\ \mu m$ size fractions. At least 300 grains were counted in every sample. Six basic classes were distinguished: lithoclasts (with mineral type when possible), volcanic glass, plant remnants, shell fragments, and benthic plus planktonic foraminiferal tests.

The CHN-O Elemental Analyser by Carlo Erba Instruments was used for total carbon content (TC) and organic carbon content (TOC) analyses. Carbonate carbon was calculated using the equation: $CaCO_3 = (TC\text{-}TOC) \cdot 8.33$ [weight %].

Heavy metals were investigated by inductively coupled plasma emission

mass spectrometry (ICP-MS, VG Plasma Quad PQ 1 equipped with a VG multi-channel analyzer) in the Institute of Geosciences, Kiel. Blank samples, drift-control samples, rock standards and duplicates were used for calibration. The measuring error estimated from independent duplicate samples was for most elements better than 5–10%. A detailed description of sample preparation techniques is given in GARBE-SCHÖNBERG (1993).

Samples for ^{210}Pb dating were taken from GBC continuously at intervals of 2 cm and 4 cm. Additional samples were taken from GC to obtain the background activity level. The fraction <63 µm was separated and homogenised. Probes of about 0.2 g were spiked with ^{209}Po and subjected to sequential acid digestion. Finally the ionic polonium was plated onto a silver planchet suspended in the leachete for approximately 4 hours. ^{210}Pb was determined by an alpha spectrometry of its grand daughter – ^{210}Po.

Results

Acoustic Surveys

Four PARASOUND profiles were surveyed in the study area (fig. 1). The composite diagram of the profile running perpendicular to the coast is presented in fig. 2. The structural features of the record are in general: a very strong bedrock reflector, a transparent sediment wedge covering the bedrock at water depths between 40 m and 100 m, and small basins filled with sediments occurring more offshore.

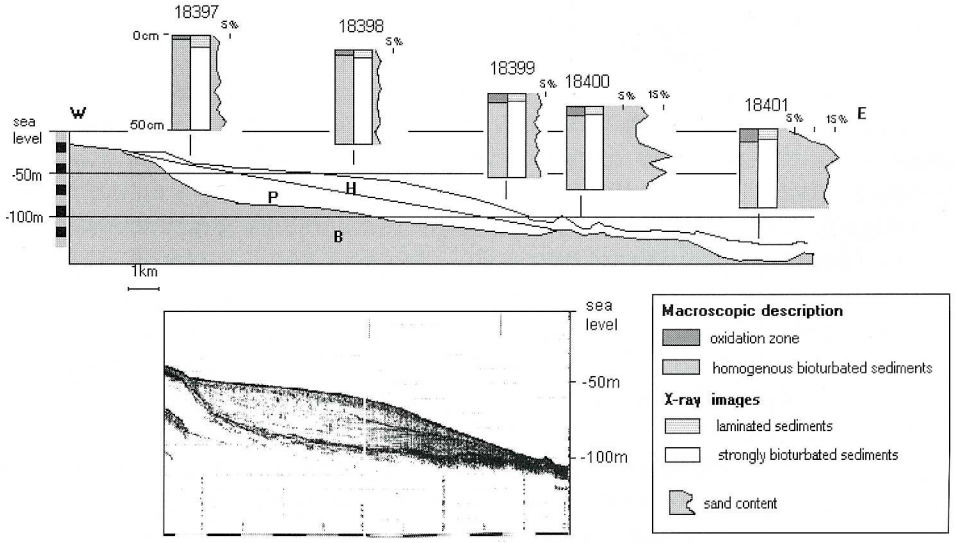

Fig. 2: Sediment logs of box cores (macroscopic, and from X-ray radiographs), and Parasound profile. See text for explanation.

From E to W, the section is as follows: In the outer shelf, where the water depth is about 150 m, seafloor bed topography is uneven and rugged. In some parts, the basement rocks are exposed on the sea bottom or are covered only with a thin blanket of modern sediments. Approaching 130–120 m depth, bigger basins are observed, filled with sediments up to 15 m thick. In the E–W direction, they are as much as 3 km long. Sampling station 18401 is located in the largest basin (depth 134 m). At water depths between 100 m and 50 m, a clastic sediment wedge develops in the landward direction. It is more than 10 km wide East–West with sediment thicknesses up to 40 m throughout the section. In the perpendicular N-S profile, which crosses the structure, the sediments are 40 m to 45 m thick. However, an unconformity is observed in the wedge, suggesting a complex evolution of sedimentation. The most modern layers are developed best as topsets and foresets with topsets dominanting. The sampling stations 18399, 18398 and 18397 were located on this sediment wedge. In shallower parts at less than 50 m depth, almost no young sediment cover is found. A strong reflector, which is supposed to be the bedrock reflector, marks the bottom. The bedrock relief has a step-like form, implicating a tectonic origin.

Three main acoustic units are distinguished (fig. 2): two acoustically transparent units H and P separated by a strong bottom reflector from the basal unit B. Unit H is composed of clays and silts probably representing the Holocene sediment cover. Unit P is truncated at its top by an unconformity, indicating the deglacial transgression surface. It consists of sediments older than the deglacial transgression. The basal unit B comprises the crystalline basement with an accentuated relief as bottom reflector at its top.

Sediment properties

The study is based on material collected from five stations (fig. 1 and 2), at water depths of 45.5 m (18397), 59 m (18398), 91 m (18399), 103 m (18400), and 133 m (18401).

The GC recovery varies between 5.32 m (18397) and 7.19 m (18398). Their lithology is uniform: homogeneous clays with patches of calcareous sand. An unconformity was reached – below which clayey sand and fine gravel deposits were found only in core 18397 at 4.8 m depth. The magnetic susceptibility is uniform for all the cores and ranges between 30–40 cgs. The detail GC reports are presented by WIESNER et al. (1999).

Mostly GBC material was used for current work. The recoveries of box cores from station 18397 offshore are 50 cm, 50 cm, 43 cm, 45 cm, and 40 cm respectively. There are two distinct layers: the surface layer (usually 1.5 cm to 7 cm – fig. 2) consisting of brown and almost fluid muddy to sandy sediments of the oxidisation zone, and the underlying layer composed of homogeneous sediments, olive-brown in colour. These sediments are often

strongly bioturbated – some patches of brown material associated with burrow infills are found below the oxidisation zone. The sediment is dominantly silty clay although in some places, patches of calcareous sand, which is also concentrated in burrows, are observed.

The detailed granulometry reveals an increase of sand and silt content in offshore direction (fig. 2). It reaches up to 16%. The grain size distribution is unimodal with maximum in coarse clay or fine silt fraction.

Water content [weight %] was between 40% and 55%. Hence the material was not investigated immediately after coring, the values represent lower boundaries. In all the GBC the results decrease from 50-55% in surface sediments to 40–50% at the bottom.

X-ray radiographs reveal several sediment structures (fig. 2, 3). In the upper 2 cm to 8 cm of all cores, a fine stratification is well developed. It is almost undisturbed by bioturbation, which is common below. Among them are open burrows, burrows filled with surrounding sediment or from the oxidisation zone laying above, backfill structures, U-shaped burrows, and some ichno-genera: *Chondrites*, *Trichichnus* and *Planolites* (BROMLEY 1990).

Coarse fraction analysis

Coarse fraction analysis was performed mostly on fraction >250 μm from samples taken every 5 cm. The 125–250 μm fraction was also studied in a couple of samples – the results obtained were similar to the fine fraction, and are shown in fig. 4.

Among planktonic foraminifera, the most common genera are *Globigerinoides*, *Neoglobuquadriana*, *Globigerina* and *Globorotalia*. Their relative abundance increases in offshore direction from about 5% up to 30% of the coarse fraction. The most frequent benthic foraminifera are *Quinqueloculina* sp, *Ammonia beccarii*, *Bolivina robusta*, *Brizalina* sp, *Hanzawaia tagaensis*, *Fursenkoina* sp, and *Bulimina* sp. The tests are very often reworked and altered. They amount to about 8–10%, only in the most offshore core up to 15–20%.

A planktonic to benthic foraminiferal ratio was calculated on the basis of the obtained data and presented in fig. 5. An increasing trend in offshore direction is observed. The averaged values for cores start with 0.66 for 18397 through 1.11 (18 398), 1.4 (18 399), 1.31 (18 400) up to 1.67 for the most offshore core 18 401.

Shell and skeleton fragments are common components of the sediments. They are often strongly reworked, especially in core 18397. Most fragments are not identifiable, among others shells of bivalves, gastropods, ostracods, and pteropods are recognised. Maximal amounts of fragments are found In bulk samples in the most onshore cores, probably because of accumulation of reworked material from shallower waters.

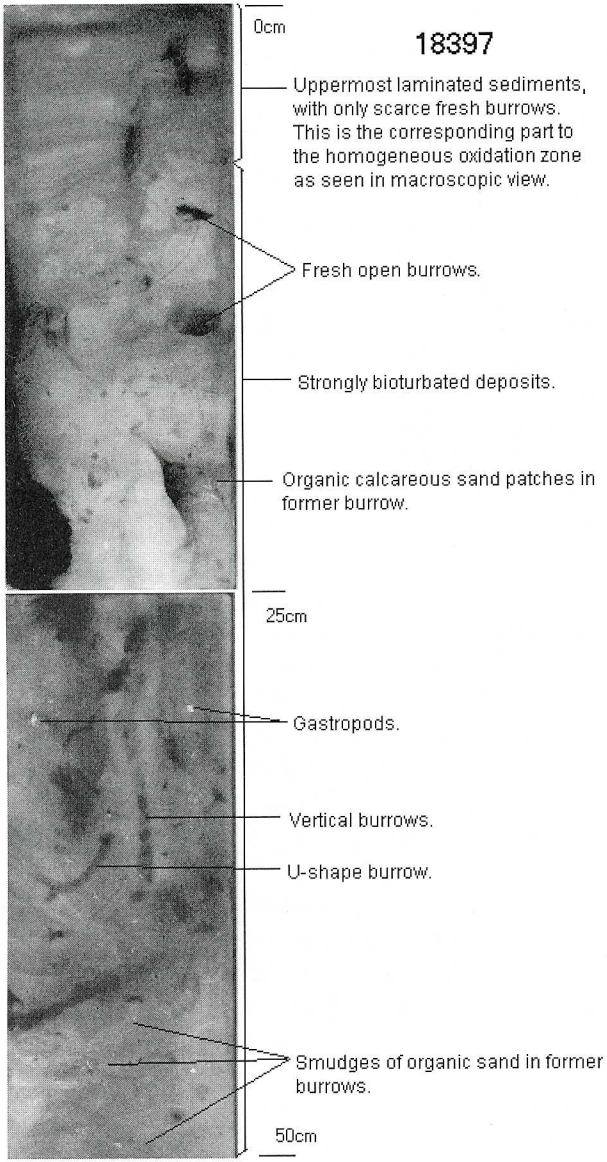

Fig. 3: X-ray radiographs from box core 18397.

Volcanic glass was also examined to find a reference level for historical eruptions. The distribution is very scarce, and its provenance is problematic.

Plant fragments lie below 10% in all the studied cores. Their distribution is relatively even.

Lithoclasts are mostly composed of aggregates of mica minerals and plant fragments, which are glued by clay minerals. They were crushed and

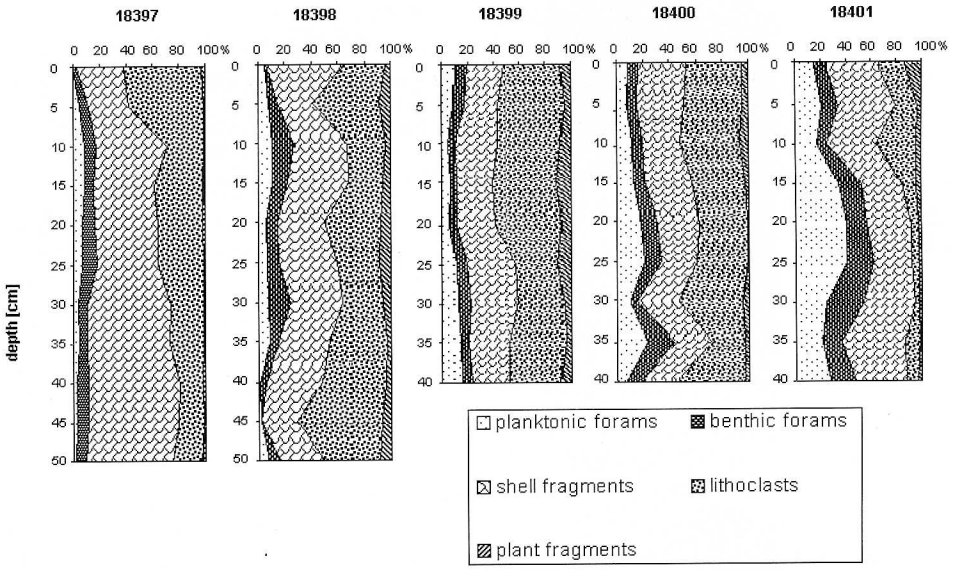

Fig. 4: Coarse fraction analyses box cores showing percentages of planktonic and benthic foraminiferas, shells and skeleton fragments, lithoclasts, and plant fragments in sediment.

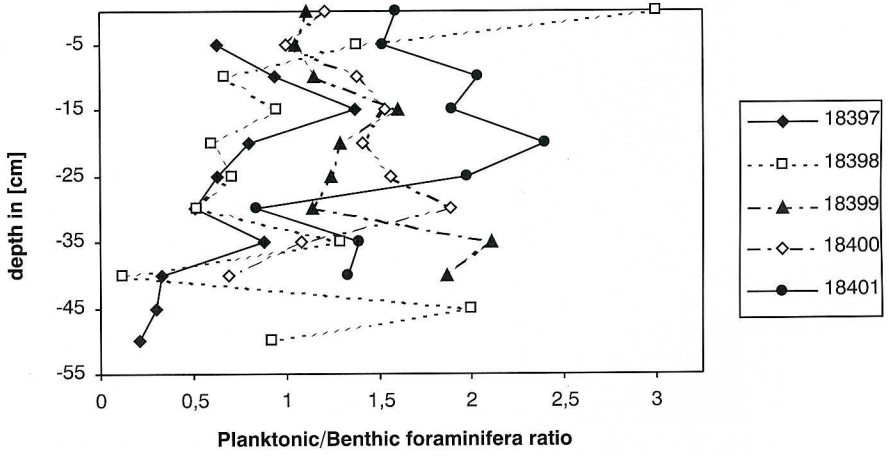

Fig. 5: Planktonic to benthic foraminiferal ratio in the sand fraction of box cores.

counted separately for coarse grain analyses. The most common minerals are muscovite and biotite, usually in aggregates. Quartz is the second abundant mineral. Grains are often subrounded to subangular, and covered by iron coatings. In core 18 400, there are exceptionally well rounded grains, which are up to 8 mm in diameter – probably redeposited from local subma-

rine sources. Feldspar and zircon were also identified, both minerals occur only rarely. The contribution of lithoclasts is significant in sediments from the clastic sediment wedge (cores 18 397-18 399), where it reaches 60%. In more offshore deposits this value is rapidly decreasing (to less than 10%).

Carbon Content

Carbon analyses reveal three parameters: the amount of total carbon, organic carbon and carbonate carbon content.

The total carbon content (TC) is in a range of 1.2 to 1.8% (fig. 6). The lowest values are in the lowermost part of 18 400 core and the highest in the most proximal 18 397. In all cores, a slight increase in TC is observed in the upper parts. Distribution along the cores is uniform with an exception of core 18 400, which is more differentiated. In cores 18 399 and 18 401, an increase in carbon content is noticed below 30 cm.

The total organic carbon (TOC) clearly shows the relationship of organic carbon content and distance from land – in the offshore direction, carbon content decreases (fig. 6). The next prominent feature is an increase in TOC in the uppermost parts – probably caused by a concentration of living organisms on or just below the sea bottom. The anomaly present in the lower part of core 18 399 is connected with a fresh bioturbation burrow, also observed in the radiograph, and in the distribution of ^{210}Pb (fig. 8).

The calculated carbonate carbon content (fig. 6) ranges between 3 and 8%. Values increase offshore with the only exception in core 18 397 (the

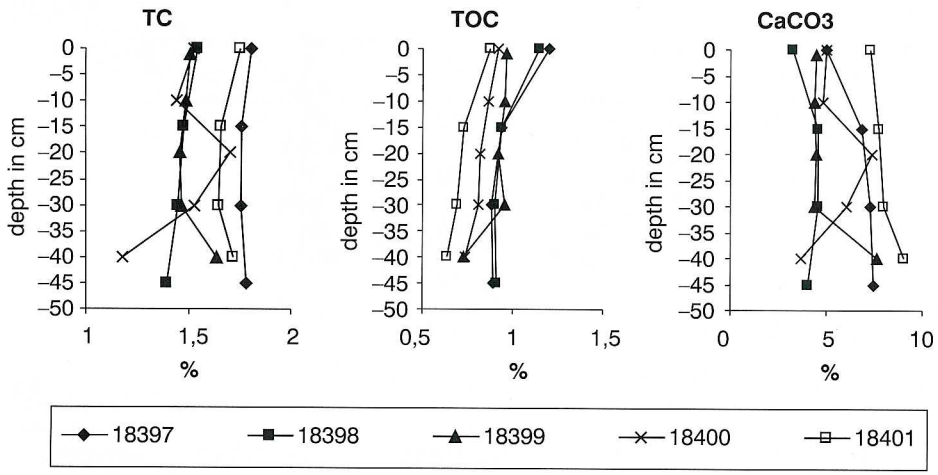

Fig. 6: Total carbon (TC), total organic carbon (TOC) and carbonate carbon ($CaCO_3$) contents in the box cores.

nearest onshore core), which is probably enriched in reworked organic carbonate material from the shallower parts of Nha Trang Bay.

Heavy metals

The following metals were investigated: Cd, Cr, Cu, Pb, and Zn. Their distribution is shown on fig. 7. All the box cores were sampled every 10 cm. The lead content varies between 24.5 and 38.4 ppm, and two trends can be observed in its distribution. The first is a vertical increase as the surface samples reveal higher values, and the second is a lateral decrease in lead content in the offshore direction. Cu values range between 14.3 pm and 22.6 ppm with a decreasing offshore trend except in core 18 397. In the uppermost part of this core an abrupt increase is observed. Both could be tied with

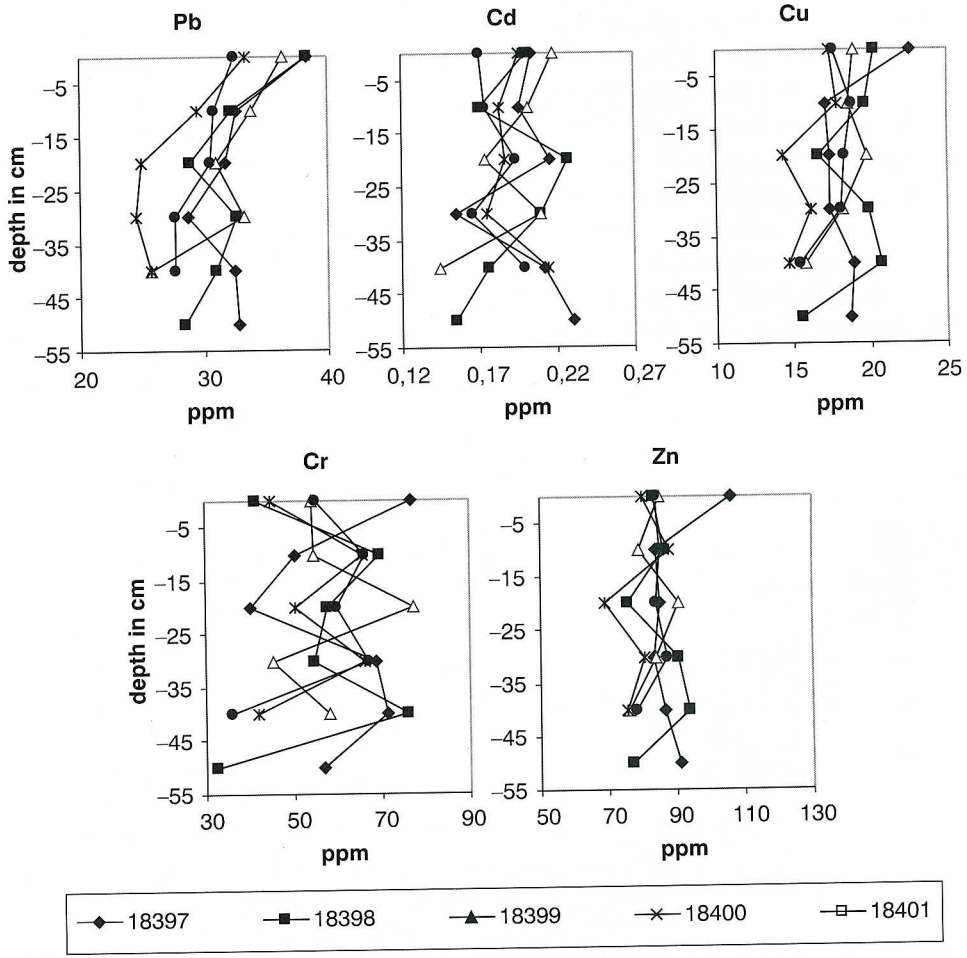

Fig. 7: Distribution of heavy metals: Pb, Cd, Cu, Cr, and Zn. Note different scales.

an increase in transport from onshore in recent years. For Cd, the extreme values are 0.14 ppm and 0.227 ppm, and for Cr 32.52 ppm and 76.7 ppm. There are no distinct patterns of distribution although the maximum value is observed in surface sediments of the nearshore core. Zn values lie between 68.8 ppm and 105.9 ppm with a slight increasing trend onshore. The highest value is in surface sample of the most nearshore core.

^{210}Pb

Two sets of samples were examined from cores 18 399 and 18 400. The maximum measured activity was above 40 dpm/g in the upper part of 18 399 and about 25 dpm/g in 18 400. The background activity level was determined to be about 2 dpm/g. The measured ^{210}Pb excess are presented in fig. 8.

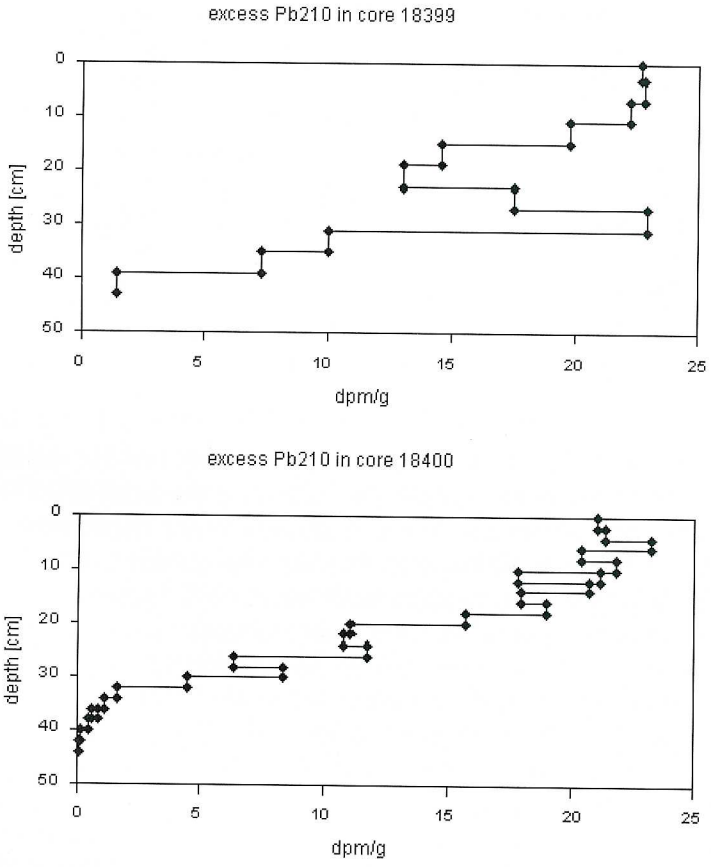

Fig. 8: Excess of ^{210}Pb in box cores 18 399 (4 cm sample ranges) and 18 400 (2 cm sample ranges).

To use this data and estimate the sedimentation rate, several assumptions must be made. The most important of them are after Nittrouer et al. 1979; Carpenter et al. 1981; Carpenter et al. 1985; and Huh & Su 1999:

- The requirement of constant deposition rate.
- Constant initial excess ^{210}Pb concentration during at least a few hundred years.
- Loss of ^{210}Pb from sediment horizons is achieved only by radioactive decay.
- Mixing is confined to the surface mixing layer (SML), and is constant with depth.
- Individual intervals of sediment used for analyses have well-defined depositional times that are short compared to the overall dating period.
- Accurate decay constant for ^{210}Pb.

From the sediment description and general knowlegde of the area, it is known that the sedimentation rate is not constant, there occurs also intensive mixing of sediments, not only in surface layer as assumed in the most of models, which requires caution in the interpretation of the data.

Sedimentation rates are calculated from gradients of excess ^{210}Pb. The linear rate model and constant flux model were considered for calculations. Using the values for water content, rates of 0.37 cm/yr (linear rate model) and 0.24 cm (constant flux model) for core 18399, and 0.33 cm/yr and 0.18 cm/yr respectively for the 18400 core were obtained. If we take a sediment-density of 2.5 g/cm^3 (Carpenter et al. 1982), sedimentation rates vary between 0.9 and 1.8 g/cm^2/yr.

Discussion and Conclusions

On the basis of the presented results, the shelf can be subdivided into three parts: the inner shelf, the middle shelf, and the outer shelf (fig. 9).

The inner shelf comprises areas of shallow water depth less than 40 m. Most of Nha Trang Bay belongs to this part. As shown by seismic surveys, there is no, or only a thin, modern sediment cover. Material is reworked by dominant processes like wave and tidal currents action, and transported offshore. Therefore, it is a sediment-bypassed area.

The middle shelf extends between 40 m and 100 m water depth. It is dominated by a clastic sediment wedge resembling a delta-like structure, which is located in position privileged by bedrock relief. Here the highest sedimentation rate is observed: as fallout from water column and as lateral transport of reworked material from the inner shelf. The latter is especially expressed in form of high participation of crushed skeleton particles. The seismic profiles reveal aggradation to be dominant – it may point to sea level rise as main factor influencing the sediment architecture. Several unconfor-

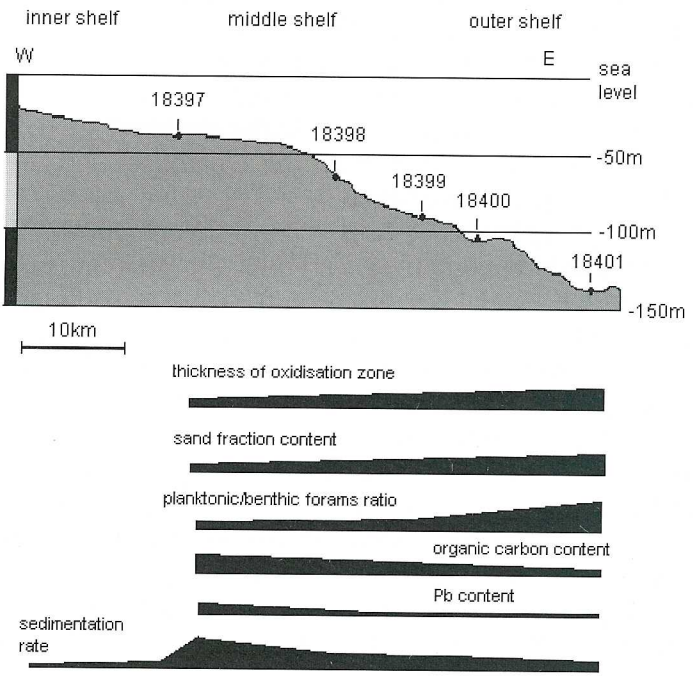

Fig. 9: The main trends observed in shelf sediments, and shelf area division.

mities in this structure suggest a geological history for this sediment body comprising the last glacial cycle.

The outer shelf shows several small basins below 100 m water depth. Fully marine conditions govern the sedimentation in this part. Deposition is concentrated in basins up to 15 km in diameter, which are created by subsurface bedrock morphology. The terrestrial material found here is significantly reworked.

Sedimentation on the shelf is concentrated only in some zones (clastic wedge, small basins). In general the whole shelf is only a bypassing area for particulate matter with temporary (i.e. hundreds to several thousands of years) sedimentation in privileged places.

The sediments are composed mainly of mud (mostly clayey silt), in accordance with the findings of Su & Wang (1994). A couple of trends related to water depth and/or distance from the shore can be distinguished in their properties (fig. 9).

Typically two zones are distinguished in the cores, an upper brown oxidation zone, and a deeper homogeneous zone, usually olive in colour. The thickness of the upper zone is only a few cm, and increases in the offshore direction.

The sand fraction increases offshore. It is composed mostly of skeletal fragments, planktonic and benthic foraminifera, and lithoclasts with lower content of plant fragments. The biogenic carbonate particles make up most of the sand fraction. Hence the organic production can be assumed as more or less uniform in the area, especially in in the middle shelf (cores 18 397–18 400). The dilution effect may explain the differences in grain size. It is caused by the predominant deposition of fine terrestrial mineral matter in the nearshore area, and by the winnowing of biogenic components.

The planktonic to benthic foraminiferal ratio shows an increasing trend in the offshore direction, in agreement with observations made by Zheng & Fu (1994) for shelf areas in the East China Sea.

The lithoclast content decreases in the coarser grain fraction further offshore. Lithoclasts are composed of mica and quartz grains – typical products of humid tropical weathering of granites, where feldspars are changed into clay minerals by chemical weathering. Since granites are the dominant basement rocks in the surroundings of Nha Trang Bay and in the source areas of rivers entering the bay, it can be concluded that the terrigenous sediments are derived mostly from this area.

Most of the mineral grains and many skeleton particles reveal traces of reworking. Since this phenomenon is most common in the shallowest cores, we suggest that winnowing and crushing of the sand fraction takes place during bypassing the inner shelf area, whereas in core 18 400 (103 m water depth) older, maybe nearshore, deposits were probably redeposited.

The organic carbon content shows an offshore directed decreasing trend. The values are about 1%, typical for shelf areas in SCS (Calvert et al. 1993; Richter 1998; Schimanski 1998). This trend points out the river-discharged matter as the main source of organic carbon in the sediment. The observed downcore decrease of organic carbon content is probably an effect of progressive decomposition of organic compounds.

The carbonate carbon values indicate an increasing trend offshore, with the exception of core 18 397, which is enriched in redeposited biogenic material. The measured values between 4 and 8% seem to be typical for this kind of sediment in the South and East China Seas (Li et al. 1991; Wang et al. 1995; Richter 1998; Schimanski 1998).

The heavy metals concentrations reference mostly the background level. A slight enrichment in the most onshore surface sediments is noted for Pb and Cr only. It can be tied with the anthropogenic impact, although the degree of change is relatively small. In comparison, Pearl River estuary sediments have at least a two-fold increase (Li et al. 2000).

All the sediments are strongly bioturbated. The identified ichnofossils are in ecological agreement with modern low-energy conditions favourable to benthic life. Very important exceptions are in the uppermost laminated part of

all cores. This can indicate a sedimentation rate much higher than the biogenic mixing rate. Concerning overall conditions (seasonality of climate, river seasonal floods etc.) periodically rapid sedimentation, which is probably related to the summer monsoon, is assumed. Organisms later bioturbate the sediment. The almost complete loss of primary stratification in the deeper parts of the cores indicates that the breaks between sedimentation events are long enough to get the whole sediment column bioturbated.

The ^{210}Pb based sedimentation rates should be taken as maximum values. Only a few authors used the ^{210}Pb dating alone (KOIDE et al. 1972; HONG et al. 1997). Other researchers using at least two parallel methods(^{137}Cs, ^{234}Th, ^{14}C, ^{239}Pu and others) found that the ^{210}Pb commonly overestimates the sedimentation rates. Reviews given by CARPENTER et al. (1982, 1985) reveal that the real values can be overestimated by 2 to 28 times. KIM & BURNETT (1988), analysing the Peru margin sediments, found the ^{210}Pb results to be 2 to 7 times higher than the sedimentation rates based on other methods (including ^{14}C). HUH & SU (1999) found for ECS sediments the ^{210}Pb rates to be 53% higher on an average than those of ^{137}Cs. SOMAYAJULU et al. (1999) also found that the method overestimates. Comparing the current results (0.2-0.4cm/yr) with others from shelf areas (e.g.: 0.39 cm/yr, KOIDE et al. 1972; 0.09 cm/yr, HONG et al. 1997), they seem to be realistic. It is therefore assumed that the error is not larger than a factor of 2-3, i.e. between 0.1 and 0.4 cm/yr. Furthermore, the only radiocarbon datings available in this part of Vietnam shelf seem to support this values. SCHIMANSKI (personal communication) obtained high long-term sedimentation rates up to 0.64 cm/year.

The maximum sedimentation rate measured by the ^{210}Pb method is 1.8 g/cm^2/yr. It can also be estimated using seismic survey data. In the most onshore long core, the unconformity separating probable Pleistocene sediments from the Holocene one was reached. Taking a time period from the sea level curve of HANEBUTH et al. (2000) for the depth of this boundary, we can estimate the total minimum sedimentation rate to be 0.04 cm/yr. When we limit the calculation only to the time when the water depth was deeper than 30 m at the locality in order to allow sedimentation of fines without bigger influence of wave action etc., values of ~0.07 cm/yr can be obtained. These numbers assume the sedimentation rate to be constant.

Concluding remarks:

– What kind of sediment is deposited in Nha Trang Bay?

It is homogeneous mud with sand content up to a few percent, composed of about 1% organic carbon and 3–8% carbonate carbon, with mica and quartz as dominant lithoclasts in the sand fraction. Biogenic carbonates are in form of foraminiferal tests, mollusc shells and other skeletal fragments.

The sediments are strongly bioturbated with the exception of the uppermost part (oxidation zone).

– What is the modern sedimentation rate?

Depending on the estimation and locality, it lies probably between 0.1 and 0.4 cm/yr, but it is not constant. These values hold only for the clastic sediment wedge covering the central shelf and small areas of sedimentation on the outer shelf In quite a large part of the shelf, only bypassing of sediment takes place.

– Which processes are affecting sedimentation the most?

Short mountainous rivers deliver most of the sediments. In the inner shelf area, the reworking and transportation of material dominates, mostly through wave action and tidal currents. In the middle and outer shelf, biogenic activity increases with both higher production and bioturbation. Bedrock relief and sea level fluctuations are also important on longer time scales.

References

Bromley, R.G. (1990): Trace Fossils. Biology and Taphonomy.– Unwin Hyman, London, 280 p.

Calvert, S.E., Pedersen, T.F. & Thunell, R.C. (1993): Geochemistry of the surface sediments of the Sulu and South China Seas.– Mar. Geol., **114**:207–231.

Carpenter, R., Bennet, J.T. & Peterson, M.L. (1981): ^{210}Pb activities in and fluxes to sediments of the Washington continental slope and shelf.– Geochim. et Cosmochim. Acta, **45**:1155–1172.

Carpenter, R., Peterson, M.L. & Bennett, J.T. (1982): ^{210}Pb-derived sediment accumulation and mixing rates for the Washington continental slope.– Mar. Geol., **48**:135–164.

Carpenter, R., Peterson, M.L. & Bennett, J.T. (1985): ^{210}Pb-derived sediment accumulation and mixing rates for the Greater Puget Sound region.– Mar. Geol., **64**:291–312.

Davis, A.M., Aitchison, J.C., Flood, P.G., Morton, B.S., Baker, R.G.V. & Haworth, R.J. (2000): Late Holocene higher sea-level indicators from the South China coast.– Mar. Geol., **171**:1–5.

Depetris, P.J. (1996): Riverine Transfer of Particulate Matter to Ocean Systems.– In: Ittekkot, V., Schäfer, P., Honjo, S. & Depetris, P.J. [eds.], Particle Flux in the Ocean, SCOPE-Report, Wiley, Chichester, **57**:53–69.

Fairbridge, R.W. (1986): Monsoons and Paleomonsoons.– Episodes, **9**:143–149.

Fontaine, H. & Workman, D.R. (1997): Vietnam.– In: Moores, E.M. & Fairbridge, R.W. [eds.], Encyclopedia of European and Asian Regional Geology, Chapman & Hall, 774–782.

Fromaget, J., Saurin, E., Arambourg, C., Blondel, F., Bonelli, F., Bourgoin, M.J., Bourret, R., Colani, M., Counillon, H., Deprat, J., Diener, C., Douville, H., Dussault, L., Giraud, J., Gubler, J., Hoffet, J.H., Jacob, C., Joubert, E., Lacroix, M.A., Lamothe, D., Lantenois, H., Mansuy, H., Patte, E., Petiton, A., Pivateau, J., Priem, F., Repelin, J., Rerolle, M.E., Zeil, G. & Zeiller, R. (1952): Carte geologique de l'Indochine.– l'Institut Geographique National, Paris.

Garbe-Schönberg, C.-D. (1993): Simultaneous determination of thirty-seven trace elements in twenty eight international rock standards by ICP-MS.– Geostand. Newsl., **10**:81–97.

Hanebuth, T. (2000): Sea-Level Changes on the Sunda Shelf during the last 50,000 years.– Ber.-Reps., Inst. f. Geowiss., Christian-Albrechts-Universität Kiel, **12**, 104 p.

HANEBUTH, T., STATTEGGER, K. & GROOTES, P.M. (2000): Rapid flooding of the postglacial Sunda Shelf – a precise sea-level record.– Science, **288**:1033–1035.

HONG, G.H., KIM, S.H., CHUNG, C.S., KANG, D.J., SHIN, D.H., LEE, H.J. & HAN, S.J. (1997): ^{210}Pb-derived sediment accumulation rates in the southwestern East Sea (Sea of Japan).– Geo-Mar. Lett., **17**:126–132.

HONG, G.H., LEE, S.H., KIM, S.H., CHUNG, C.S. & BASKARAN, M. (1999): Sedimentary fluxes of ^{90}Sr, ^{137}Cs, ^{239,240}Pu and ^{210}Pb in the East Sea (Sea of Japan).– The Science of the Total Environment, **237/238**:225–240.

HUANG, Q.-Z., WANG, W.-Z. & CHEN, J.-C. (1994a): Tides, tidal currents and storm surge set-up of South China Sea.– In: ZHOU D., LIANG, Y.R., & ZENG, C. [eds.], Oceanology of China Seas, Kluwer, Dordrecht, **1**:113–122.

HUANG, Q.-Z., WANG, W.-Z., LI, Y.S. & LI, C.W. (1994b): Current characteristic of the South China Sea.– In: ZHOU D., LIANG, Y.R., & ZENG, C. [eds.], Oceanology of China Seas, Kluwer, Dordrecht, **1**:39–47.

HUH, C.A. & SU, C.C. (1999): Sedimentation dynamics in the East China Sea elucidated from Pb-210, Cs-137 and Pu-239, Pu-240.– Mar. Geol., **160**:183–196.

KIM, K.H. & BURNETT, W.C. (1988): Accumulation and biological mixing of Peru margin sediments.– Mar. Geol., **80**:181–194.

KOIDE, M., SOUTAR, A. & GOLDBERG, E.D. (1972): Marine geochronology with ^{210}Pb.– Earth Planet. Sci. Lett., **14**:442–446.

LI, C., CHEN, G., YAO, M. & WANG, P. (1991):The influences of suspended load on the sedimentation in the coastal zones and continental shelves of China.– Mar. Geol., **96**:341–352.

LI, X., WAI, O.W.H., LI, Y.S., COLES, B.J., RAMSEY, M.H. & THORNTON, I. (2000): Heavy metal distribution in sediment profiles of the Pearl River estuary, South China.– Appl. Geochem., **15**:567–581.

MILLIMAN, J.D. & MEADE, R.H. (1983): World-wide delivery of river sediment to the oceans.– J. Geol., **91**:1–21.

MILLIMAN, J.D. & SYVITSKI, J.P.M. (1992): Geomorphic/tectonic control of sediment discharge to the ocean: The importance of small mountainous rivers.– J. Geol., **100**:525–544.

NITTROUER, C.A., STERNBERG, R.W., CARPENTER, R. & BENNETT, J.T. (1979): The use of Pb-210 geochronology as a sedimentological tool: application to the Washington continental shelf.– Mar. Geol., **31**:297–316.

PIRAZZOLI, P.A. (1991): World atlas of Holocene sea-level changes.– Elsevier, Amsterdam, 300 p.

SHAW, P.T., & CHAO, S.Y. (1994): Surface circulation in the South China Sea.– Deep-Sea Res. I, **41**:1663–1683.

SIMKIN, T., SIEBERT, L., MCCLELLAND, L., BRIDGE, D., NEWHALL, C. & LATTER, J.H. (1981): Volcanoes of the world.– Hutchinson Ross, Stroudsburg, 233 p.

SOMAYAJULU, B.L.K., BHUSHAN, R., SARKAR, A., BURR, G.S. & JULL, A.J.T. (1999): Sediment deposition rates on the continental margins of the eastern Arabian Sea using ^{210}Pb, ^{137}Cs and ^{14}C.– The Science of the Total Environment, **237/238**:429–439.

STATTEGGER, K., KUHNT, W., WONG, K., BÜHRING, C., HAFT, C., HANEBUTH, T., KAWAMURA, H., KIENAST, M., LORENC, S., LOTZ, B., LÜDMANN, T., LURATI, M., MPHLHAN, N., PAULSEN, A.-M., PAULSEN, J., PRACHT, J., PUTAR-ROBERTS, A., HUNG, N., RICHTER, A., SALOMON, B., SCHIMANSKI, A., STEINKE, S., SZAREK, R., NHAN, N., WEINELT, M., & WINGUTH, C. (1997): Sequence stratigraphy, late Pleistocene– Holocene sea level fluctuations and high resolution record of the post-

Pleistocene transgression on the Sunda Shelf. Cruise Report Sonne 115, Sundaflut.– Ber.-Reps., Geol.-Pal. Inst., Christian-Albrechts-Universität Kiel, **86**, 211 p.

SU, G. & WANG, T. (1994): Basic characteristic of modern sedimentation in South China Sea.– In: ZHOU D., LIANG, Y.R., & ZENG, C. [eds.], Oceanology of China Seas, Kluwer, Dordrecht, **2**:407–418.

TJIA, H.D. (1980): The Sunda Shelf, Southeast Asia.– Z. f. Geomorp., **24**/4:405–427.

TJIA, H.D. & LIEW, K.K. (1996): Changes in tectonic stress field in northern Sunda Shelf basin.– In: HALL, R. & BLUNDELL, D. [eds], Tectonic Evolution of Southeast Asia., Geol. Soc. Spl. Publ., **106**:291–306.

VIETNAM: POINTE LAGAN TO CAP VARELLA (1997).– British Crown Nautical Map, Admiralty Publ., London.

WANG, L., SARNTHEIN, M., ERLENKEUSER, H., GRIMALT, J., GROOTES, P., HEILIG, S., IVANOVA, E., KIENAST, M., PELEJRO, C. & PFLAUMANN, U. (1999): East Asian monsoon climate during the Late Pleistocene: high-resolution sediment records from the South China Sea.– Mar. Geol., **156**:245–284.

WANG, P., WANG, L., BIAN, Y. & ZHIMI, J. (1995): Late Quaternary paleoceanography of the South China Sea: surface circulation and carbonate cycles.– Mar. Geol., **127**:145–165.

WIESNER, M.G., STATTEGGER, K., KUHNT, W., ARPA, C., BRACKER, E., CATANE, S., LEON, M.DE, DUYANEN, J., FABER, U., GERBICH, C., HESS, S., HOLBOURN, A., JAGODZINSKI, R., KAMINSKI, M., KAWAMURA, H., KRÜGER, O., LORENC, S., NGUYEN HUU SUU, NGUYEN HUY PHUC, NGUYEN VAN BACH, PAULSEN, H., PELEO-ALAMPAY, A., RICHTER, A., RIMEK, R., SCHIMANSKI, A., SEEMAN, B., SHARMA, C., SIRINGAN, F., STEEN, E., STEINKE, S., SZAREK, R., SZCZUCIŃSKI, W., VO DUY SON, WERSCH, V.VON, WETZEL, A. & WITZKI, D. (1999): Late Pleistocene-Holocene sea level fluctuations and high-resolution stratigraphy of the post-Pleistocene Transgression of the Vietnam Shelf. Particle fluxes and recolonisation of the 1991 Mount Pinatubo tephra layer in the South China Sea. Cruise Report SONNE 140, Südmeer III.– Ber.-Reps., Inst. f. Geowiss., Christian-Albrechts-Universität Kiel, **7**, 157 p.

WIESNER, M.G., ZHENG, L., WONG, H.K., WANG, Y. & CHEN, W. (1996): Fluxes of particulate matter in the South China Sea.– In: ITTEKKOT, V., SCHÄFER, P., HONJO, S. & DEPETRIS, P.J. [eds.], Particle Flux in the Ocean. SCOPE-Report, Wiley, Chichester, **57**:293–312.

ZHENG, S. & FU, Z. (1994): Foraminiferal faunal trends in China seas.– In: ZHOU D., LIANG, Y.R., & ZENG, C. [eds.], Oceanology of China Seas, Kluwer, Dordrecht, **1**:255–274.

Unpublished

RICHTER, A. (1998): Die Auswirkung des spätpleistozänen Meeresspiegelanstiegs auf Sedimentationsprozesse im Paläo-Mekong Delta.– M.Sc. Thesis, Inst. f. Geowiss., Christian-Albrechts-Universität Kiel, 134 p.

SCHIMANSKI, A. (1998): Diversität und Entwicklung von Faziesräumen auf dem Sunda Schelf im Verlauf der Postpleistozänen Transgression.– M.Sc. Thesis, Inst. f. Geowiss., Christian-Albrechts-Universität Kiel, 63 p.

WYRTKI, K. (1961): Scientific results of marine investigation of the South China Sea and Gulf of Thailand.– Naga Report, **2**,195 p.

Manuskript eingegangen am: 19.03.2001
Revidiert am: 21.06.2001